

Melting and multipole deformation of sodium clusters

 A. Rytönen, H. Häkkinen^a, and M. Manninen

Department of Physics, University of Jyväskylä, P.O. Box 35, FIN-40351 Jyväskylä, Finland

Received: 1 September 1998 / Received in final form: 10 December 1998

Abstract. Melting and multipole deformations of sodium clusters with up to 55 atoms are studied using an *ab initio* molecular dynamics method. The melting temperature regions for Na₂₀, Na₄₀, and Na₅₅⁺ are estimated. The melting temperature region determined here for Na₅₅⁺ agrees with the one determined experimentally. The dominating deformation type observed at the liquid phase for Na₂₀ and Na₄₀ is octupole deformation and for Na₁₄ and Na₅₅⁺ quadrupole deformation.

PACS. 36.40.Cg Electronic and magnetic properties of clusters – 36.40.Ei Phase transitions in clusters – 36.40.Mr Spectroscopy and geometrical structure of clusters

Melting and structural properties of small clusters have been studied intensively during the last years using various numerical and experimental techniques [1–3]. Recent introduction of *ab initio* methods for studying geometric and electronic structure in alkali metal clusters [4–6], along with tight-binding calculations and molecular dynamics simulations with many-body potential [7, 8], has provided new detailed information about their finite-temperature properties. In our recent study [6], electronic and structural properties of Na₄₀ were studied using an *ab initio* method [9]. Na₄₀ was found to melt around 300–350 K and was found to be dominantly octupole deformed.

Development in experimental cluster physics has enabled the study of melting transition in metal clusters with less than 100 atoms. Melting temperatures of sodium clusters with 55–200 atoms were determined experimentally recently [10–12]. The results of *ab initio* calculations and experiments of melting behaviour of small sodium clusters can now be compared directly.

In this paper we have studied the finite-temperature dynamics of sodium clusters containing 8–55 atoms, including both electronic and structural properties, with *ab initio* BO-LSD-MD (Born-Oppenheimer Local-Spin-Density Molecular Dynamics) method devised by Barnett and Landman [9]. Both magic and non-magic clusters were included in the study. The melting temperature regions obtained here for Na₂₀, Na₄₀ and Na₅₅⁺ were found to increase monotonically as a function of particle number. For smaller sodium clusters with 8, 10, and 14 atoms, however, a melting temperature region could not be convincingly identified with traditional indicators. Na₂₀ and Na₄₀ were principally octupole deformed at the whole temperature region studied. Na₁₄ was found to be prolate at 50–450 K,

and Na₅₅⁺ was prolate at temperatures above its melting region.

In the BO-LSD-MD method, the Kohn-Sham (KS) one-electron equations for the single-electron states of the valence electrons are solved for a given nuclear configuration of the ions. From the converged solution the Hellmann-Feynman forces to the ions are calculated, which together with the classical Coulomb repulsion between the positive ion cores determine the total forces to the ions, according to which classical molecular dynamics for the ions is performed. The fully converged solution for the electronic structure is obtained for each successive ionic configuration. The current implementation uses plane waves combined with fast Fourier transform techniques as the basis for the one-electron wave functions and norm-conserving, non-local, separable [13] pseudopotentials by Troullier and Martins [14, 15] to describe the valence electron – ion interaction, and the LSD parametrization by Vosko, Wilk, and Nusair [16].

The deformations of clusters were analyzed in terms of a multipole expansion [17]. Dimensionless shape parameters S_l defined as

$$S_l = \sum_{m=-l}^l |a_{lm}|^2 = \sum_{m=-l}^l \frac{4\pi(2l+1)}{9r_s^{2l} N^{2l/3+2}} |Q_{lm}|^2, \quad (1)$$

were employed to determine the strength of each multipole component. The multipole moments Q_{lm} are defined as

$$Q_{lm} = \sqrt{\frac{4\pi}{2l+1}} \int d^3r r^l Y_{lm}(\theta, \phi) n(\mathbf{r}), \quad (2)$$

where Y_{lm} is a spherical harmonic, $n(\mathbf{r})$ is the valence electron density, and r_s is the density parameter of the electron gas. The details of this formulation are presented in [17]. When defined in this way, all possible values of m are included in each S_l , making it rotationally invariant. The

^a Present address: School of Physics, Georgia Institute of Technology, Atlanta, GA 30332, USA

shape parameters are calculated during a molecular dynamics run for $l=2, 3$ and 4 corresponding to quadrupole, octupole and hexadecupole deformations of the cluster, respectively.

The kinetic temperature of each cluster was slowly raised by scaling the velocities of the ions. A heating rate of 5 K/ps was used for each cluster size. For Na_8 , Na_{20} , and Na_{40} also a lower heating rate of 2.5 K/ps was used. Two traditional melting characteristics were used to determine the melting region: (i) latent heat in the energy vs. temperature curve and (ii) the diffusion coefficient, defined as

$$D = \frac{1}{6} \frac{R^2}{s}, \quad (3)$$

where R^2 is the mean square displacement of the ions calculated with respect to the positions of the ions in the beginning of a time period s ($= 4 \text{ ps}$). When the cluster is solid, its diffusion coefficient is small, and as the cluster melts, the diffusion coefficient increases to a value comparable to the one typical for bulk liquid.

The simulations for each cluster were started from a configuration known or anticipated to be a low-energy structure. The starting configuration for Na_8 was the dodecahedron (D_{2d} symmetry), well established to be the lowest energy structure found for Na_8 along with the archimedean antiprism (D_{4d}) [4]. For Na_{10} , the bicapped antiprism, the lowest energy structure found in [4], was employed. The simulation study for Na_{14} was started from a prolate structure [18] consisting of three stacked squares, the middle one rotated by $\pi/4$ with respect to the others, and two atoms at the ends. The starting configuration for Na_{55}^+ was a complete icosahedron from which one electron was removed. The starting structure for Na_{40} [6] was constructed from a 55 atom perfect icosahedron by removing all the 12 corner atoms and one (111) facet. This structure, however, was observed to spontaneously transform into an energetically more favorable structure having fivefold symmetry [6]. One should note that the simulations described here for Na_{40} are the same as in [6]. The heating simulation for Na_{20} was started from a low energy structure suggested in [4], consisting of three decahedra on top of each other rotated by $\pi/5$, minus the topmost atom plus two atoms around the central decahedron. This structure is in fact the inner part of the favorable structure of Na_{40} [6].

Figure 1 shows the diffusion coefficient of the clusters heated at 5 K/ps calculated over time periods of 4 ps for clusters with 14 atoms or more. For each cluster, the diffusion coefficient displays values less than $0.3 \times 10^{-5} \text{ cm}^2/\text{s}$ at low temperature, but as the temperature increases, the values for the diffusion coefficient increase to values typical for bulk liquid sodium (over $2 \times 10^{-5} \text{ cm}^2/\text{s}$). The temperature region where the diffusion coefficient starts to increase may be interpreted as the melting region.

The melting temperature regions deduced from the potential energy vs. temperature curves were in accord with the ones deduced from the diffusion coefficient for Na_{20} , Na_{40} and Na_{55}^+ , but for Na_{14} , the potential energy vs. temperature curve did not show any distinct transition region. For smaller clusters, Na_8 and Na_{10} , neither of the indica-

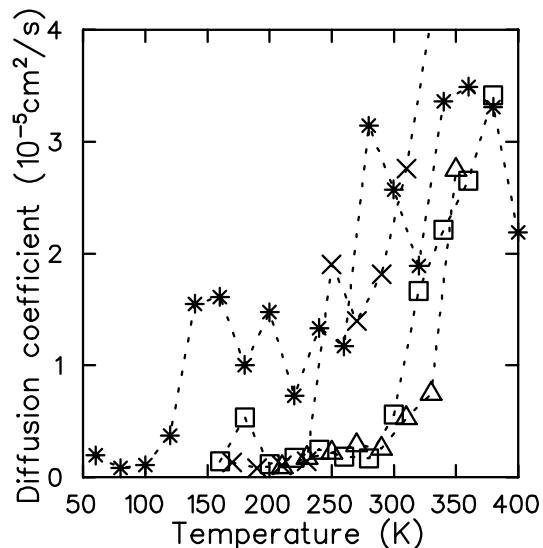


Fig. 1. The diffusion coefficient calculated over time periods of 4 ps and plotted as a function of the average temperature in each time period. Stars, crosses, open squares, and open triangles represent the simulation results for Na_{14} , Na_{20} , Na_{40} , and Na_{55}^+ , respectively.

tors used revealed any clear transition region. These clusters exhibit only isomerisation [6]. The diffusivity of Na_{14} corresponds to liquid phase at temperatures higher than 250 K , but an estimate for the melting temperature region could not be determined.

It is well known that the melting transition is rounded in finite systems, and as the particle number of the system decreases, the melting region is broadened [19]. During a single heating simulation, the melting transition may happen anywhere inside the melting region, and thus an accurate numerical determination of the melting region would require either averaging over a large number of simulations or making one simulation with an extremely low heating rate. For small clusters having wide melting region, other methods might produce more accurate results (for example [20]). However, from our simulations, reasonable estimates for the melting regions can be obtained. Na_{20} was observed to melt around 250 K when it was heated with a rate of 5 K/ps . When heated at a lower rate of 2.5 K/ps , the transition appeared more rounded and had a finite width of approximately $235\text{--}275 \text{ K}$. Na_{40} was observed to melt around 300 K when heated at 5 K/ps , and at 350 K when heated at 2.5 K/ps . Na_{55}^+ showed a rounded transition at a temperature region of $310\text{--}360 \text{ K}$.

For the cluster sizes studied, the melting temperature region seems to be a monotonous function of particle number. It has to be noted, however, that Na_{20} and Na_{40} are magic electronically. It is likely that the melting temperature regions of non-magic clusters at this size region could be lower than those determined here [21].

Schmidt *et al.* [11] have recently determined experimentally the melting temperatures of sodium clusters with $70\text{--}200$ atoms. Our *ab initio* calculations for small sodium clusters with up to Na_{55}^+ give higher melting temperatures than

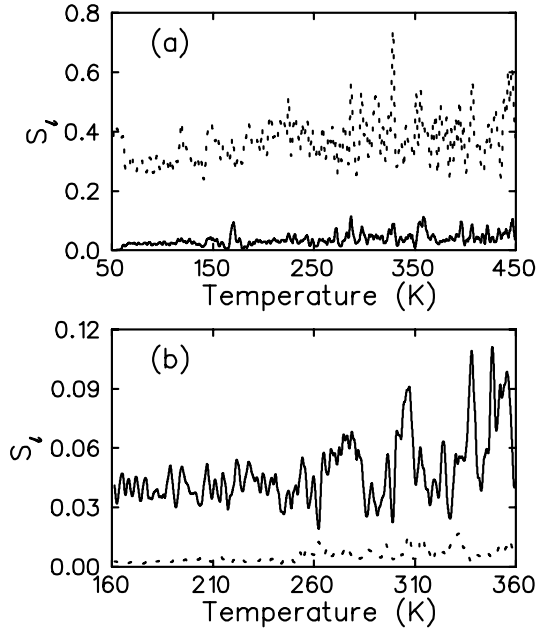


Fig. 2. Shape parameter vs. temperature of (a) Na_{14} and (b) Na_{20} for quadrupole ($l = 2$, dotted curve) and octupole ($l = 3$, solid curve) deformation.

those obtained experimentally in [11] for somewhat larger clusters. It is possible that the heating rates used here are too high, resulting in a delay in the melting transition of the system, observed earlier for example for Lennard-Jones clusters of comparable size [22]. However, the melting temperature region deduced here for Na_{55}^+ agrees with the one determined experimentally [12].

Figure 2(a) shows the shape parameters S_l , $l=2, 3$, for Na_{14} as a function of temperature. At the whole temperature region studied, the dominating deformation type is quadrupole deformation, and by examining the principal moments of inertia, it is found that the structure is prolate. This agrees with earlier observations [23]. Figure 2(b) shows the corresponding parameters for Na_{20} . The dominating deformation type for Na_{20} is octupole deformation, like for Na_{40} [6]. Even though the ground state structure for Na_{20} in the jellium picture is a sphere, it is very soft against octupole deformation [25]. Consequently, this will be the dominant deformation at finite temperature. Our findings for Na_{20} are in agreement with the finite temperature results of Röthlisberger and Andreoni [4]. The hexadecupole deformation (not shown) was very small for Na_{14} and about half of the value for octupole deformation for Na_{20} .

For Na_{40} it was observed [6] that much before melting the cluster spontaneously transforms from the structure based on the icosahedral order into a structure lower in energy and with a larger HOMO-LUMO gap, and with enhanced octupole deformation. A nearly similar structure has also been observed in tight-binding calculations [24]. The octupole deformation was found to be the dominating deformation type in both solid and liquid phase [6].

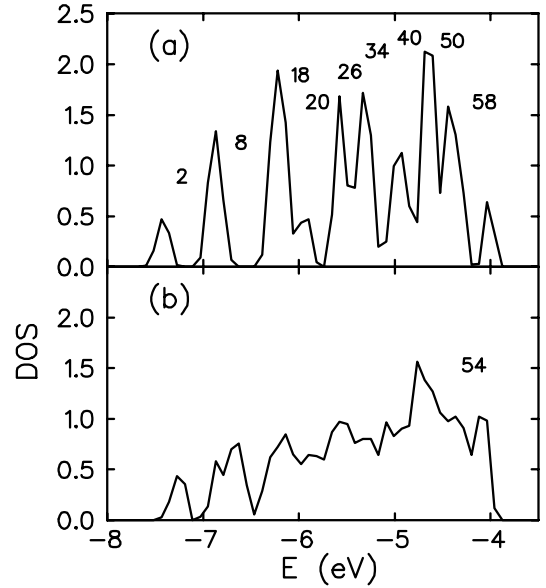


Fig. 3. Density of KS states of Na_{55}^+ for (a) icosahedral cluster, (b) melted cluster. The numbers indicate the total number of states below the underlying minimum.

The simulation of Na_{55}^+ was started from a perfect icosahedron. The structure of Na_{55}^+ as a function of temperature was studied with a modified cosine parameter method, based on the angles between position vectors of neighbouring atoms, described in [22]. By applying this method, Na_{55}^+ was found to retain its icosahedral structure at low temperatures, and the icosahedral order was observed to be destroyed as the cluster melted. Figure 3 displays the distribution of KS states at temperature regions lower and higher than the melting temperature region for Na_{55}^+ . At low temperature, where the cluster is icosahedral and essentially spherical, the KS states display a clear jellium type shell structure, split by the icosahedral symmetry. However, there is no HOMO-LUMO gap. This behaviour strongly suggests that an icosahedron is not the ground state structure for Na_{55}^+ . As the cluster melts and the icosahedral order is destroyed, the electronic structure loses almost completely its spherical jellium type characteristics, Fig. 2(b). At this stage, the cluster tends to open a HOMO-LUMO gap, shown as the last minimum at the curve in Fig. 2(b). By examining the principal moments of inertia of the cluster it was found that the liquid Na_{55}^+ is clearly prolate, as predicted by the jellium model [25].

The sodium clusters studied here from Na_{14} to Na_{55}^+ all show some kind of deformation at temperatures high enough for the cluster to display liquid characteristics. This demonstrates quite convincingly that liquid metal clusters are not spherical in general. This is in agreement with the picture given by *ab initio* calculations of Röthlisberger and Andreoni [4] for sodium clusters with up to 20 atoms.

In summary, we have studied melting and structural deformations of sodium clusters with 8 to 55 atoms with an *ab initio* molecular dynamics method. Na_{20} was observed to melt around 235–275 K, Na_{40} around 300–350 K and

Na_{55}^+ around 310–360 K. For smaller clusters, melting temperature regions could not be estimated. The melting temperature region obtained here for Na_{55}^+ agrees with the one determined experimentally [12]. Liquid Na_{14} and Na_{55}^+ are prolate, while Na_{20} and Na_{40} exhibit enhanced octupole deformation.

This work was supported by the Academy of Finland.

References

1. J.D. Honeycutt, H.C. Andersen: *J. Phys. Chem.* **91**, 4950 (1987); B. Raoult, J. Farges, M.F. De Feraudy, G. Torchet: *Philos. Mag. B* **60**, 881 (1989); J.P. Rose, R.S. Berry: *J. Chem. Phys.* **98**, 3246 (1993); O.B. Christensen, K.W. Jacobsen: *J. Phys.: Condens. Matter* **5**, 5591 (1993); Q. Wang, M.P. Iniguez, J.A. Alonso: *Z. Phys. D* **31**, 299 (1994); C.L. Cleveland, U. Landman, W.D. Luedtke: *J. Phys. Chem.* **98**, 6272 (1994); S. Valkealahti, M. Manninen: *J. Phys.: Condens. Matter* **9**, 4041 (1997); Y. Oshima, K. Takayanagi: *Z. Phys. D* **27**, 287 (1993); T.P. Martin, U. Näher, H. Schaber, U. Zimmermann: *J. Chem. Phys.* **100**, 2322 (1994)
2. W.A. de Heer: *Rev. Mod. Phys.* **65**, 611 (1993)
3. M. Brack: *Rev. Mod. Phys.* **65**, 677 (1993)
4. U. Röthlisberger, W. Andreoni: *J. Chem. Phys.* **94**, 8129 (1991)
5. V. Bonačić-Koutecký, J. Jellinek, M. Wiechert, P. Fantucci: *J. Chem. Phys.* **107**, 6321 (1997)
6. A. Rytönen, H. Häkkinen, M. Manninen: *Phys. Rev. Lett.* **80**, 3940 (1998)
7. R. Poteau, F. Spiegelmann, P. Labastie: *Z. Phys. D* **30**, 57 (1994)
8. A. Bulgac, D. Kusnezov: *Phys. Rev. B* **45**, 1988 (1992)
9. R.N. Barnett, U. Landman: *Phys. Rev. B* **48**, 2081 (1993)
10. M. Schmidt, R. Kusche, W. Kronmüller, B. von Issendorff, H. Haberland: *Phys. Rev. Lett.* **79**, 99 (1997).
11. M. Schmidt, R. Kusche, B. von Issendorff, H. Haberland: *Nature* **393**, 238 (1998)
12. R. Kusche, T. Hippler, M. Schmidt, B. von Issendorff, H. Haberland: *Eur. Phys. J. D, ISSPIC* **9**
13. L. Kleinman, D.M. Bylander: *Phys. Rev. Lett.* **48**, 1425 (1982)
14. N. Troullier, J.L. Martins: *Phys. Rev. B* **43**, 1993 (1991)
15. A kinetic energy cutoff $E_C^{\text{PW}} = 5.6$ Ry is used for the plane-wave basis set
16. S.H. Vosko, L. Wilk, M. Nusair: *Can. J. Phys.* **58**, 1200 (1980); S.H. Vosko, L. Wilk: *J. Phys. C* **15**, 2139 (1982)
17. M. Koskinen, P.O. Lipas, M. Manninen: *Z. Phys. D* **35**, 285 (1995)
18. A. Yoshida, T. Døssing, M. Manninen: *J. Chem. Phys.* **101**, 3041 (1994)
19. H. Reiss, P. Mirabel, R.L. Whetten: *J. Phys. Chem.* **92**, 7241 (1988); H.-P. Cheng, X. Li, R.L. Whetten, R.S. Berry: *Phys. Rev. A* **46**, 791 (1992)
20. J. Jellinek, S. Srinivas, P. Fantucci: *Chem. Phys. Lett.* **288**, 705 (1998)
21. S. Valkealahti, M. Manninen: *Comp. Mater. Sci.* **1**, 123 (1993)
22. A. Rytönen, S. Valkealahti, M. Manninen: *J. Chem. Phys.* **108**, 5826 (1998)
23. H. Häkkinen, M. Manninen: *Phys. Rev. B* **52**, 1540 (1995)
24. F. Spiegelmann, R. Poteau: *Comments At. Mol. Phys.* **31**, 395 (1995)
25. B. Montag, Th. Hirschmann, J. Meyer, P.-G. Reinhard, M. Brack: *Phys. Rev. B* **52**, 4775 (1995)